Available online at www.sciencedirect.com

ScienceDirect

Procedia CIRP 58 (2017) 73 – 78

www.elsevier.com/locate/procedia

16th CIRP Conference on Modelling of Machining Operations

Cutting simulations using a commercially available 2D/3D FEM software for forming.

Eric Segebade[a,]*, Michael Gerstenmeyer[a], Frederik Zanger[a], Volker Schulze[a]

[a]*wbk – Institute of Production Science, Karlsruhe Institute of Technology (KIT), Kaiserstr. 12, 76131 Karlsruhe, Germany*

* Corresponding author. Tel.: +49-721-608-45906 ; fax: +49-751-608-45004. E-mail address: eric.segebade@kit.edu

Abstract

Chip formation simulations require either sophisticated material based element removal or deactivation routines, or a powerful remeshing procedure. Therefore the accuracy of all chip formation simulations significantly depends on the FEM-software as well as the material data. Over the course of the past years, a few select commercial programs became the pre-eminent choice for chip formation simulations. In this work, the software simufact.forming, which is not one of those few programs widely in use, has been employed for 2D and 3D chip formation simulations. Orthogonal cutting experiments with AISI4140 were conducted and subsequently modeled, including the cutting edge radius. The results were analyzed with regard to how well chip formation and the resulting process forces in 2D and 3D can be depicted.

Peer-review under responsibility of the scientific committee of The 16th CIRP Conference on Modelling of Machining Operations

Keywords: Finite element methid (FEM); Cutting, Chip formation

1. Introduction

The modeling and simulation of cutting operations is steadily gaining momentum in terms of its utility for predicting macroscopic part performance. Various models from various scientific institutes and companies can already predict the cutting forces, temperatures, microstructural and phase changes, residual stresses, tool wear, tool life, and even chip type for machining operations [1-6].

Several software applications are most widely used for FEM- simulations of cutting operations (alphabetical order):

- Abaqus
- Advantedge
- Ansys/LS-Dyna
- Deform
- Forge

There are also some non-commercial custom programs and program modifications in use.

In addition to FEM-simulations, meshless techniques [7] and smooth particle hydrodynamics (SPH) [8] can also be used to depict the cutting processes of various materials. Chip formation can be simulated within FEM via different strategies, such as element deletion, node separation, continuous or discontinuous re-meshing, or by a combination of these. As shown in [9], the friction models and coefficients chosen profoundly influence the quality of simulations (regardless of software) and remain a critical factor for depicting cutting in simulations. Many of these methods have been evaluated by [10], who conclude that the simulation predictions vary widely depending on the software package, the modeling strategy, and (using the same software) the user. An even more detailed benchmark of simulation software for cutting processes is planned over the next few years within the scope of a CIRP collaborative work.

Future refinements in the FEM-simulations of cutting operations will focus on the incorporation of: physics-based material models (e.g., those considering microstructure), friction models obtained with cutting-relevant experimental data, thermal conductivity models, workpiece state data that accounts for upstream processing, cutting edge microgeometries, tool roughness, and wear data. Improvements in 3D simulations and computation speed – particularly when simulating complete parts – are also areas of interest.

Peer-review under responsibility of the scientific committee of The 16th CIRP Conference on Modelling of Machining Operations
doi:10.1016/j.procir.2017.03.195

Even though advanced cutting simulations usually focus on the resulting surface integrity details, such as residual stresses and microstructural changes, the first step in model validation is to predict the cutting forces for a range of process parameters. Without realistic cutting forces, the resulting predicted surface integrity can hardly be considered physically correct – barring the possibility of fitting prediction models to experimental data using incorrectly calculated forces (and, in turn, incorrectly calculated stress, deformation and possibly temperature fields). The asymmetry of the cutting edge should also be considered, since experience shows that edge asymmetry not only influences process forces [11] but also the resulting surface integrity of parts [12]. According to the literature, a change in the edge segment length at the flank face S_α will likely impact the process forces more severely than a change in the edge segment length of the rake face S_γ [13].

In this work, a 2D and 3D orthogonal cutting model is set up using the commercial FEM-software *simufact.forming*. The software specializes in forming and joining operations and has not previously been used for chip formation simulation. Following a brief analysis of the system's sensitivity to cutting edge asymmetry, an investigation of friction parameters is conducted. Finally, the model is tested against experimental cutting force data obtained for different process parameters with AISI 4140 considering the real cutting edge microgeometries.

2. Experiments

2.1. Experimental setup

Orthogonal cutting experiments with AISI 4140 QT were carried out on a Karl Klink vertical broaching machine. Workpieces with dimensions of 80*x*4*x*20 *mm* with the depth of cut applied to the height of 20 *mm* were used. While the workpiece is moved vertically, the tool is fixed on a three component dynamometer Type Z 3393 by Kistler. A rake angle of -7° was used for all experiments. All experiments were repeated three times. Additionally a new characterized cutting edge was used for each set of parameters. The three sets of process parameters are listed in Table 1.

Table 1. Orthogonal cutting experiments with AISI 4140 QT

set no.	cutting velocity v_c in m/min	uncut chip thickness h in µm		
1	80	25	50	100
2	100	25	50	100
3	150	25	50	100

2.2. Cutting tools and cutting edge characterization

Uncoated Walter Tools cutting inserts type WKM P8TN 6028833 with a cutting wedge angle of 90° and thus a flank angle of 7°. The inserts were shipped with a nominal cutting edge radius of 40 ± 10 μm. Each edge was analyzed using a confocal light microscope of the NanoFocus AG and subsequently characterized by the form-factor method [14]. The form-factor K is the ratio of edge segment lengths S_γ at the rake face and S_α at the flank face. The mean size of the radius $\overline{S}$ is the arithmetic mean of S_γ and S_α. Table 2 shows the combinations of tool microgeometry and experiment. It is notable, that none of the cutting edges features a K equal to or smaller than 1. All edges exhibit a S_γ that is at least 10% longer than the respective S_α.

Table 2. Cutting edge radii of the WKM P8TN 6028833

cutting velocity v_c in m/min	uncut chip thickness h in µm	mean cutting edge radius $\overline{S}$ in µm	form-factor K
80	25	35.0	1.8
80	50	35.0	1.1
80	100	41.0	1.2
100	25	44.0	1.3
100	50	38.5	1.6
100	100	39.5	1.5
150	25	33.5	1.2
150	50	44.0	1.4
150	100	39.0	1.7

3. FE-Simulations

3.1. 2D-FE-Model

2D-FE-simulations were set up with two different accuracy settings henceforth referred to as "basic" and "normal". The basic setup features approximately three times bigger elements than the normal setup. The basic setup was used for the comprehensive friction coefficient study. The normal setup as shown in Fig. 1 was compared with the experimental data as well as the sensitivity analysis regarding cutting edge asymmetry. In all cases the length of cut was set as 1 *mm*. The workpiece was modeled with a length of 4 *mm* and a thickness of 1 *mm*.

The mesh type "Quadtree" in plane strain condition with continuous remeshing depending on refinement boxes was used. The number of elements varied with uncut chip thickness with the highest number of elements necessary for 100 μm of uncut chip thickness. In the example shown in Fig. 1 (uncut chip thickness of 100 μm) the number of elements increased with length of cut from 15000 to up to 85000 elements.

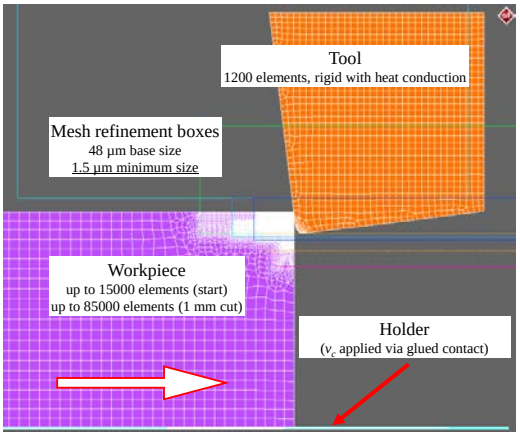

Fig. 1. 2D-cutting model (normal accuracy)

3.2. 3D-FE-Model

For 3D-FE-simulations both hexahedral and tetrahedral meshes were used. In case of the hexahedral mesh the elements are distributed between the base element edge length of 120 μm and the minimal edge length of 7.5 μm. The initial number of elements of 66000 increases with length of cut up to 254000 elements at 1.0 *mm* length of cut. The tetrahedral mesh features a base element edge length of 100 μm and a minimal edge length of 5 μm. Concurrent with the 2D-FE-simulations the number of elements necessarily increased with uncut chip thickness. Due to a sharp increase in element count and failed remeshing no refinement boxes were used for the tetrahedral mesh. The setup of the 3D-hex simulation is depicted in Fig. 2.

The workpiece was modeled with 1 *mm* in depth to the dimensions of the 2D-setup. Using a symmetry plane half of the experimental setup is depicted. This measure to reduce computational time is not suspected to reduce accuracy more than a significantly coarser mesh, which would have been necessary otherwise. All simulations were computed without parallelization on a desktop PC.

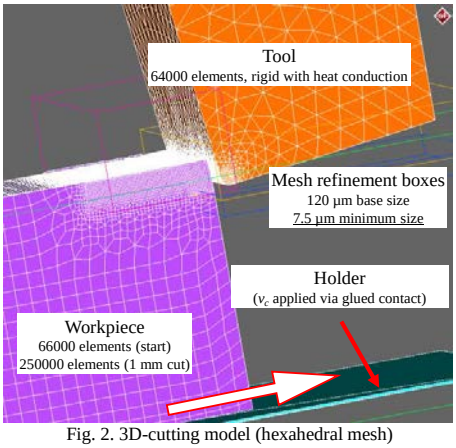

Fig. 2. 3D-cutting model (hexahedral mesh)

3.3. Material model and boundary conditions

The software works with numerous fortran-based subroutines of different functionalities. For this study the subroutine “user_fstress” was used to implement a physics based material model according to [16-18] for the workpiece. The model suggests the flow stress σ to be composed of a thermal component ($\sigma^*(T,\dot{\varepsilon})$) and an athermal component (σ_G). Dependency on temperature T and strain rate $\dot{\varepsilon}$ is considered as shown in Eq. 1.

$$\sigma = \underbrace{\sigma_0^* \cdot \left(1-\left(\frac{T}{T_0}\right)^n\right)^m}_{\sigma^*} + \underbrace{\left(\sigma_{G0} + \left(\sigma_1 + \theta_1 \cdot \bar{\varepsilon}_p\right) \cdot \left(1-\exp\left(-\frac{\theta_1 \cdot \bar{\varepsilon}_p}{\theta_0}\right)\right)\right) \cdot \frac{G(T)}{G(0K)} \cdot g(T,T_{tr})}_{\sigma_G} \quad (1)$$

The thermal component $\sigma^*(T,\dot{\varepsilon})$ considers short range dislocation obstacles with regard to temperature T, strain rate $\dot{\varepsilon}$ and the material constants n and m. Lowering the temperature as well as increasing strain rate increases the thermal component $\sigma^*(T,\dot{\varepsilon})$. Above a set temperature (T_0) the thermal component ceases to influence the flow stress. T_0 is defined as

$$T_0 = \frac{\Delta G_0}{k_B \ln\left(\frac{\dot{\varepsilon}_0}{\dot{\varepsilon}_p}\right)} \quad (2)$$

with the free activation enthalpy ΔG_0 and the Boltzmann constant k_B.

Long range dislocation obstacles are considered through the athermal component σ_G. It is mostly independent of the temperature T and considers the shear modulus G. With the term $g(T,T_{tr})$ high temperature softening is considered depending on the transition temperature T_{tr}. It is defined as 1 for $T \leq T_{tr}$. For $T > T_{tr}$. $g(T,T_{tr})$ is defined as

$$g(T,T_{tr}) = \left(1-\left(\frac{T-T_{tr}(\bar{\varepsilon}_p)}{T_m - T(\bar{\varepsilon}_p)}\right)^{\xi}\right)^{\varsigma} \quad (3)$$

with

$$T_{tr}(\bar{\varepsilon}_p) = \vartheta_0 + \Delta\vartheta \cdot \ln\left(1+\frac{\bar{\varepsilon}_p}{\dot{\varepsilon}_n}\right) \quad (4)$$

and the material constants ϑ_0, $\Delta\vartheta$, ξ, ς and the melting temperature T_m. The model has already been validated for cutting simulations in numerous works using Abaqus (e.g. [15]). The workpiece was defined as elasto-plastic.

The tool is modeled as rigid with heat conduction (transport coefficient at the interface: 10^8 $Wm^{-2}K^{-1}$). Both bodies initial temperature is set to 293°*K*. A heat transfer coefficient to the environment of 50 $Wm^{-2}K^{-1}$ and temperature dependent emissivity from 0.02 at 293.15°*K* to 0.55 at 1273.15°*K* is defined.

The tool is fixed in space while the workpiece is moved through a glued contact with a moving rigid “holder”. The software offers forging press kinematics (which are mostly not relevant for cutting), tabular data or subroutine to realize tool-movements. For this study a constant velocity in one direction was modeled with a hydraulic press.

The software allows the definition of temperature dependent coulomb friction, combined coulomb-shear friction and subroutine implementation of friction laws. In this study a temperature independent combined coulomb-shear friction model was used. The friction coefficients were varied as per Table 2. Parameter range was chosen according to past experience [15], which suggests a value of μ = 0.35 for coulomb friction for AISI4140 and uncoated cutting tools. The study was conducted using the basic accuracy and the cutting edges and process parameters as listed in Table 2. A total of 81 simulations were run for the friction study.

Table 3. Full-factorial friction coefficient study

coulomb factor µ	shear factor m
0.25	0.5
0.35	0.7
0.45	0.9

3.4. Cutting edge microgeometries

In order to study the sensitivity regarding cutting edge asymmetry, simple asymmetric cutting edges were created. The

edges feature a K of 2 and 0.5 with a $\overline{S}$ of 45 μm. Additionally two symmetrical cutting edges with r_β = 30 μm and 60 μm were used. The simulations were conducted in 2D, with low coulomb friction (μ = 0.1). The low, constant friction coefficient ensures reduced influence of the contact length on the cutting forces. Instead, the microgeometry-dependent ploughing influences the forces most strongly. With this effect predicted correctly, the simulation will be suitable for future works considering surface integrity details dependent on cutting edge microgeometry.

For the force comparison with the experiments, all measured cutting edges as listed in Table 2 were recreated and used for the corresponding process parameters in 2D and 3D.

4. Results and discussion

4.1. Sensitivity to cutting edge asymmetry

In Fig. 3 the process forces of the four different cutting edges analyzed in this study are shown. As literature suggests, asymmetric cutting edges result in higher forces in general, with a more pronounced influence of change in the flank face edge segment S_α due to ploughing. It can be deduced, that the simulation results show sensitivity of the correct tendency for cutting edge microgeometries regarding the process forces.

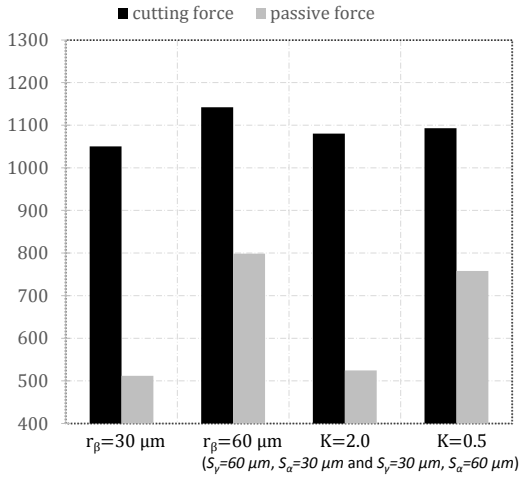

Fig. 3. 2D-simulation of cutting and passive forces with symmetrical and

4.2. Friction coefficient study

The coefficients of the full-factorial study were rated by the sum of error squares across the whole field considering both, cutting and passive force. The rating is shown in Table 4. The lowest error was observed using the parameters μ = 0.35 and m = 0.7. The difference in accuracy is small for the first three parameter sets, but increases down the list. The parameters found correspond well to what can be found in literature. Better results might be obtained with an additional study near the three sets rated best. In the end, a temperature, relative velocity and pressure dependent model should result in higher accuracy. With 8 simulations running at the same time on one desktop PC, the time required for computation was roughly 30 hours.

Table 4. Modeled coefficients of friction rating regarding process forces

coulomb coefficient μ	shear coefficient m	rating
0.35	0.7	1
0.35	0.5	2
0.45	0.5	3
0.35	0.9	4
0.25	0.5	5
0.25	0.9	6
0.25	0.7	7
0.45	0.7	8
0.45	0.9	9

4.3. Force comparison simulations - experiments

Before conducting the simulation study with the normal setup, the influence of element size on cutting forces was analyzed. The simulation modeled with 25 μm chip thickness and cutting speed of 150 m/min was run with different element sizes up to a length of cut of 1 mm. Simulations with significantly different element sizes (from 12 to 0.75 μm) yielded comparable cutting forces, as shown in Fig 4. The element size of the normal setup was considered to be sufficient and time efficient.

All further results shown in this chapter were modeled using the friction coefficients of μ = 0.35 and m = 0.7 and normal accuracy. Steady state was reached after approximately 0.4 mm length of cut. Fig. 5 to 7 show the results in comparison with the experiments. The 3D-simulations with a tetrahedral mesh are farthest off in all cases. Most forces are severely underestimated using this mesh type. It is therefore not a good choice for setting up cutting simulations with this software. Apart from the bad results, the tetrahedral mesh also requires a high number of restarts due to instabilities.

2D-simulations and 3D-simulations using the hexahedral mesh slightly overestimate the cutting force for small uncut chip thickness. At higher uncut chip thickness, the cutting force is predicted accurately. Contrary to this trend, the passive force is accurate for small uncut chip thickness, but underestimated for high uncut chip thickness at low speed. The reason for this could be an underestimation of the frictional force applied to the rake face, which should scale with uncut chip thickness. This effect is enhanced by low temperatures at this interface.

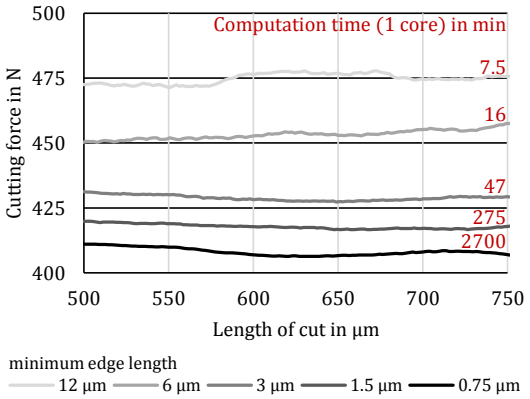

Fig. 4. Influence of element size on simulated cutting force and computation time by minimum edge length

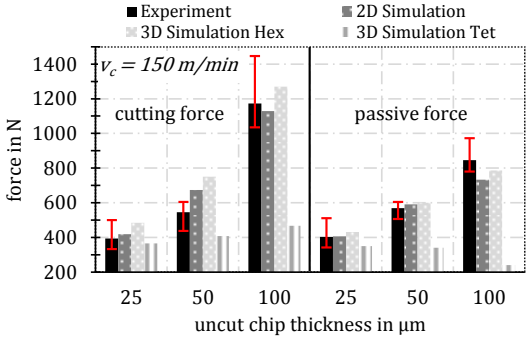

Fig. 5. Experimental and simulated process forces at *150 m/min* for uncut chip thicknesses of *25* to *100 µm*

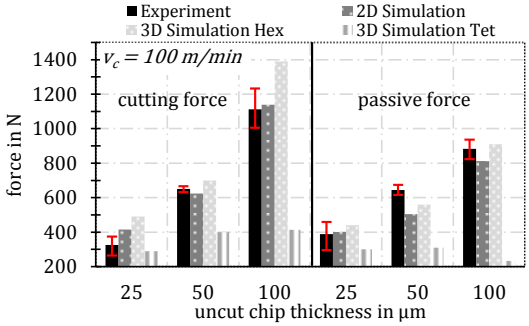

Fig. 6. Experimental and simulated process forces at *100 m/min* for uncut chip thicknesses of *25* to *100 µm*

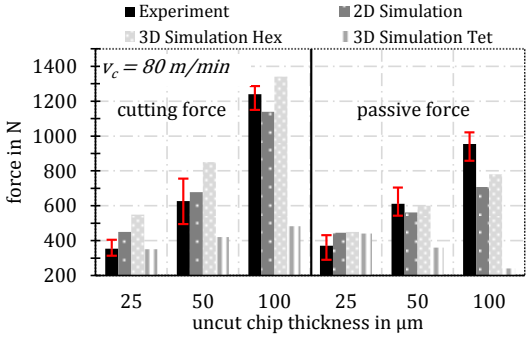

Fig. 7. Experimental and simulated process forces at *80 m/min* for uncut chip thicknesses of *25* to *100 µm*

On the one hand, a higher interface temperature should lead to higher friction coefficients and thus higher frictional forces. On the other hand, higher speeds should decrease frictional forces [15]. As can be seen in Fig. 8 and 9, the simulations show the tendency of rising interface temperature with both, uncut chip thickness and cutting speed. The temperature and speed independent friction model and its coefficients can therefore not depict all circumstances present at the tool chip interface across the simulations. Validation of the model regarding the predicted temperatures remains subject of future work including measurement of temperatures during experiments. Still, the temperatures as shown in Fig. 8 and 9 seem reasonable for dry machining.

In Fig. 10 (cutting force) and Fig. 11 (passive force), the results of the 2D-simulations were plotted on the experimental data considering a deviation of 20%. It is apparent, that all of the forces are predicted with a deviation of slightly below 20%, if the experimental data variance is considered.

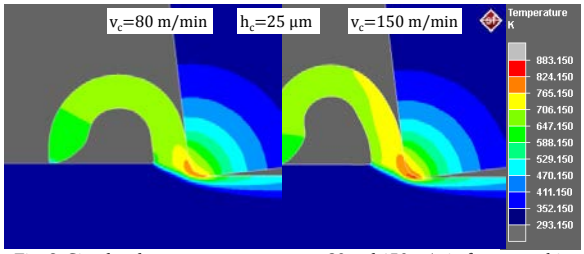

Fig. 8. Simulated process temperatures at *80* and 150 m/min for uncut chip thicknesses of *25 µm*

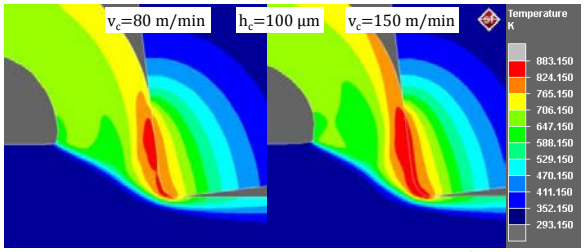

Fig. 9. Simulated process temperatures at *80* and 150 m/min for uncut chip thicknesses of *100 µm*

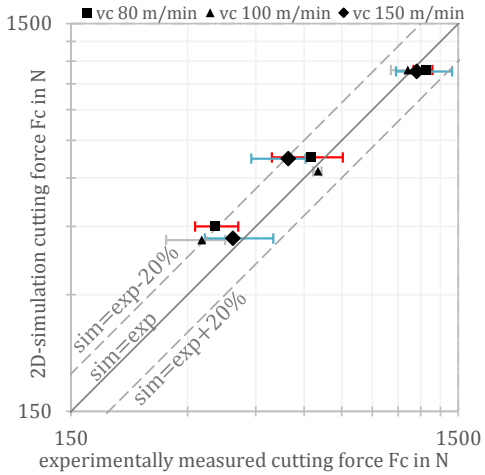

Fig. 10. Cutting forces of the 2D-simulations vs. experimental cutting forces

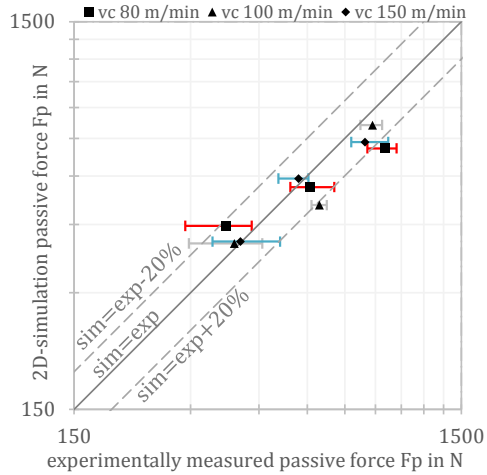

Fig. 11. Passive forces of the 2D-simulations vs. experimental passive forces

5. Conclusion and outlook

In this work, a commercial FEM-software for forming operations was used for 2D and 3D (orthogonal) chip formation simulation. The software has not previously been used for this kind of simulation.

To reflect material behavior, a constitutive material model for AISI 4140 was implemented as subroutine. Following the demonstration of sensitivity for cutting edge microgeometry, suitable friction parameters for a coulomb-shear model were found. Subsequently the change in forces due to mesh size was analyzed in a convergence study. Thusly a computing-time efficient mesh size with sufficient accuracy was chosen.

For comparison with experimental data, orthogonal cutting experiments at three different uncut chip thicknesses and speeds were conducted. FEM-models of the experiments were set up in 2D and 3D using both, hexahedral and tetrahedral mesh for 3D-simulations. All models included the measured cutting edge asymmetry.

2D-simulations reflect experimental results within *20%* deviation. 3D-simulations with hexahedral mesh yield similar results but tend to overestimate the cutting forces. 3D-simulations with tetrahedral mesh do not yield relevant results.

The software offers fast and stable simulations in 2D and 3D (3D-hexahedral, 1 mm length of cut, 48 hours). The flexible meshing and remeshing options enable submicron element edge lengths, and various remeshing options in both 2D and 3D. Single-core PC-computing requires a relatively coarse mesh in 3D-simulations due to available RAM and computation time. It is expected, that parallelization will reduce computation times considerably.

The software itself is easy to use and focused on its target processes like forming and joining operations. This results in standard-settings which are usually not usable for chip formation simulations. The ability to customize the software with Fortran-based subroutines may alleviate this shortcoming. Subroutine features include material behavior, friction models, heat-transfer, phase transitions, damage models and many more. It can therefore gain relevance for advanced modelling and analysis of chip formation processes and process-chains. Whether or not this potential can be tapped will have to be proven in future investigations.

After confirming correct force calculation, the next step will be focusing on temperatures. The interdependence of friction and temperature will require implementing a more complex friction model. Thusly the predictability of surface integrity features like residual stresses, grain refinement and phase transitions will be undertaken. This will include multi-cut simulations and 3D-simulations of turning processes. These may require high performance computing to accurately model the surface integrity features mentioned above. Finally, the modeling of serrated chip formation with this software will be explored.

Acknowledgements

The authors would like to thank Juo Son, who contributed to the programming of the material subroutine during his master thesis.

References

[1] Arrazola PJ, Özel T, Umbrello D, Davies M, Jawahir IS. Recent advances in modelling of metal machining processes. CIRP-Annals Manufacturing Technology 2013;62:695-718.
[2] Outeiro JC, Umbrello D, M'Saoubi R. Experimental and numerical modelling of the residual stresses induced in orthogonal cutting of AISI 316L steel. International Journal of Machine tools and Manufacture 2006;46:1786-1794.
[3] Filice L, Umbrello D, Micari F, Settineri L. On the finite element simulation of thermal phenomena in machining processes. Advanced Methods in Material Forming 2007:263-278
[4] Schulze V, Zanger F. Development of a simulation model to investigate tool wear in Ti-6Al-4V alloy machining. Advanced Materials Research 2011;223:535-544.
[5] Leopold J. Approaches for modelling and simulation of metal machining – a critical review. Manufacturing Review 2014;1:7.
[6] Attanasio A, Ceretti E, Fiorentino A, Cappellini C, Giardini C. Investigation and FEM-based simulation of tool wear in turning operations with uncoated carbide tools. Wear 2010;269:344-350.
[7] Uhlmann E, Gerstenberger R, Kuhnert J. Cutting simulation with the meshfree finite pointset method. Procedia CIRP 2013;8:391-396.
[8] Nam J, Kim T, Wook Cho S. A numerical cutting model for brittle materials using smooth particle hydrodynamics. International Journal Manufacturing Technology 2016;82:133-141.
[9] Malakizadi A, Hosseinkhani Km Mariano E, Ng E, Del Prete A, Nyborg L. Influence of friction models on FE simulation results of orthogonal cutting process. International Journal Advanced Manufacturing Technology 2016:1-16.
[10] Outeiro JC, Umbrello D, M'Saoubi, Jawahir IS. Evaluation of present numerical models for predicting metal cutting performance and residual stresses. Machining Science and Technology 2016;19:183-216.
[11] Bassett E, Köhler J, Denkena B. On the honed cutting edge and its side effects during orthogonal turning operations of AISI 1045 with coated WC-Co inserts. CIRP Journal Manufacturing Science and Technology 2012;5:108-126.
[12] Segebade E, Zanger F, Schulze V, Influence of different asymmetrical cutting edge microgeometries on surface integrity. Procedia CIRP 2016;45:11-14.
[13] Denkena B, Lucas A, Bassett E, Effects of the cutting edge microgeometry on tool wear and its thermo-mechanical load. CIRP Annals Manufacturing Technology 2011;60:73-76.
[14] Denkena B, Reichstein M, Brodehl J, de Leon Garcia L. Surface Preparation, Coating and Wear Performance of Geometrically Defined Cutting Edges. 8th CIRP International Workshop on Modeling of Machining Operations, (2005) May 10–11(Chemnitz).
[15] Schulze V, Michna J, Zanger F, Faltin C, Maas U, Schneider J. Influence of cutting parameters, tool coatings and friction on the process heat in cutting processes and phase transformations in workpiece surface layers. Journal Heat Treatment and Materials 2013;68:22-31.
[16] Tomé CN, Canova GR, Kocks UF, Christodoulou N, Jonas J. The relationship between macroscopic and microscopic strain hardening in F.C.C. polycrystals. Acta metallurgica 1984;32:1637-1653.
[17] Voce E. The relationship between stress and strain for homogeneous deformation. Journal of the Institute of Metals 1948;74:537-562.
[18] Authenrieth H. Numerische Analyse der Mikrozerspanung am Beispiel von normalisiertem C45E. Karlsruhe Institute of Technology, Dissertation, (2010).